

The understanding of the penetration and clusterization of 1-alkanol in bilayer membrane: An open outlook based on atomistic molecular dynamics simulation

Anirban Polley*

*Shanmugha Arts, Science, Technology and Research Academy,
Tirumalaisamudram, Thanjavur, Tamilnadu 613401, India*

(Dated: June 2, 2025)

1-alkanols are well known to have anesthetic and penetration properties, though the mode of operation remains enigmatic. We perform extensive atomistic molecular dynamics simulation to study the penetration of 1-alkanols of different chain lengths in the dioleoyl-phosphatidylcholine (DOPC) bilayer model membrane. Our simulations show that the depth of penetration of 1-alkanol increases with chain length, n , and the deuterium order of the DOPC tail increases with the chain length of the acyl-chain of the 1-alkanol. We find a cut-off value for the length of the acyl-chain of 1-alkanol, $n = 12$, where 1-alkanol with a chain length greater than the cut-off value takes longer to penetrate the membrane. Our simulation study also demonstrates that the membrane exhibits clusters of 1-alkanols with acyl chains longer than the cut-off value, whereas 1-alkanols with acyl-chain shorter than the cut-off value are distributed homogeneously in the membrane and penetrate the membrane in a shorter time than longer-acyl-chain 1-alkanols. These findings add to our understanding of the anomalies in anesthetic molecule partitioning in the cell membrane and may have implications for general anesthesia.

I. INTRODUCTION

General anesthesia [1] is a well-known phenomenon, and anesthetics are widely used in hospitals for all painless surgical procedures. However, the molecular level of understanding in the mechanism of general anesthesia is not yet understood. It is still debatable whether general anesthesia is caused directly by the binding of anesthetics to specific proteins [2, 3] and blocking the protein's function by changing conformation, or whether it is caused indirectly by a lipid-mediated mechanism [4–6] while the anesthetics alter the membrane properties such as the total volume of the membrane, the volume occupied by the anesthetics within the membrane, the phase transition temperature of lipids, the lipid chain order, membrane thickness, or the lateral pressure profile of the membrane.

Apart from anesthesia, 1-alkanol has been well known as a penetration enhancer for the transdermal drug delivery. However, the mechanism of penetration enhancers is still unknown. It is interesting to know that 1-alkanol as anesthetics exhibits the 'cutoff effect'. The anaesthetic potency of 1-alkanols is increased up to a certain cut-off chain length (dodecanol), and 1-alkanols with a chain length greater than the cutoff length have no anesthetic potency [7].

Several experimental studies have been conducted to explore the effect of the anesthetics on the properties of the lipid membrane, such as NMR spectroscopic studies that show ethanol molecules having a disordering effect on the lipids [8–13] and X-ray studies that reveal ethanol having the potential to change the lipid membrane properties such as thickness above its main phase transition

temperature [14–16]. A few molecular dynamics studies have also been performed to study the influence of the anesthetics on the lipid membrane [11, 17–28].

In the present work, using an atomistic molecular dynamics (MD) simulation technique, we investigate the penetration of 1-alkanols with varying chain lengths in a symmetric DOPC lipid bilayer membrane.

The article is arranged as follows: we first discuss the details of the atomistic molecular dynamics simulations of the bilayer membrane. Next, we present our main results of the partitioning of 1-alkanols; the deuterium order parameter of DOPC acyl chain; the penetration time of 1-alkanols; the clusterization of 1-alkanols; and the radial distribution. We end by summarizing our findings.

II. METHODS

Initial configurations of Model membrane:

We use atomistic molecular dynamics simulations (MD) with *GROMACS-2025.1* [29] to investigate 1-alkanols ($C_nH_{2n+1}OH$) of varying chain-lengths: $n = 2$ (ethanol), 5 (pentanol), 8 (octanol), 10 (decanol), 12 (dodecanol), 14 (tetradecanol) and 16 (hexadecanol) in DOPC bilayer membrane. *PACKMOL* [30] is used to build the initial configuration of symmetric DOPC lipid bilayer membrane of 256 lipids in each leaflet (with a total 512 lipids) and 16384 water molecules (such that the ratio of water to lipid is 32 : 1) to hydrate the bilayer membrane. We add 128 number (25% of total number of lipids) of 1-alkanols with $n = 2, 5, 8, 10, 12, 14, 16$ uniformly in both sides of the water layers of the symmetric bilayer membrane, respectively and study total 8 bilayer membranes without and with 1-alkanols, respectively.

Force fields:

The force field parameters of DOPC are taken from the previously validated united-atom description [17, 31–

* anirban.polley@gmail.com

34]. We have taken the same previously used force-field parameters for the 1-alkanol of different chain-lengths [17, 35–38]. In our simulation study, we use the improved extended simple point charge (SPC/E) model to simulate water molecules, with an extra average polarization correction to the potential energy function.

Choice of ensembles and equilibration:

We simulate all 8 symmetric bilayers in the NVT ensemble for 50 ps using a Langevin thermostat to avoid bad contacts caused by steric constraints, and then in the NPT ensemble for 1000 ns ($1\mu s$) ($T = 296$ K (23° C), $P = 1$ atm). To collect enough data, we repeat the simulations 4 times (for a total of $4\mu s$) for each system. We run the simulations in the NPT ensemble for the first 100 ns using Berendsen thermostat and Berendsen barostat, then remaining simulations using Nose-Hoover thermostat and the Parrinello-Rahman barostat to produce the correct ensemble using a semi-isotropic pressure coupling with the compressibility of 4.5×10^{-5} bar $^{-1}$ for the simulations in the NPT ensemble, long-range electrostatic interactions by the reaction-field method with cut-off $r_c = 2$ nm, and the Lennard-Jones interactions using a cut-off of 1 nm [32, 34, 39–41].

III. RESULTS AND DISCUSSION

To confirm that we have attained a thermally and chemically equilibrated bilayer membrane, we calculate the time evolution of the total energy of the system and the area of the lipid (shown in Fig. S1 in Supplementary Information (SI)), exhibiting asymptotic behavior with a very small fluctuation assuring an equilibrated bilayer membrane [17, 32, 39].

We begin our simulation with the initial configuration, in which lipids are homogeneously mixed and 1-alkanols are in the aqueous layers of both sides of the bilayer membrane, and simulate for $1\mu s$ to obtain an equilibrated patch of the bilayer membrane, which we analyse to determine 1-alkanol and membrane properties.

A. Density of 1-alkanol in membrane

The density profiles of the head group and the tail of the 1-alkanol for varying chain lengths have been shown in Fig 1 (a) and (b), respectively. The atoms of the 1-alkanol's $-OH$ group are considered the head group, while the atoms in the acyl chains, $-(CH_2)_{n-1}-CH_3$ with $n = 2, 5, 8, 10, 12, 14, 16$ are considered the 1-alkanol's tail. As in our simulation, $z - axis$ represents the normal to the surface of the membrane lying in the xy -plane, so the densities of the head and tail of the 1-alkanol are plotted on the z -axis. The density profiles of DOPC lipids without and with 1-alkanols are shown in Fig. S2 in SI. The density profile of the head group of 1-alkanol in Fig. 1 (a) shows that two peaks of the leaflets are exhibited at the same z -values in both leaflets,

respectively. The density profile of the tail of 1-alkanol in Fig. 1 (b) shows that two peaks are getting closer with the increasing acyl chain length. *As a result, we find that the penetration of 1-alkanol increases with the length of acyl chain of the 1-alkanol, n .*

B. Deuterium order of DOPC acyl chain

The deuterium order parameter, S_{cd} , of the acyl chains of the DOPC lipid in the membrane without and with 1-alkanol is calculated as $S_{cd} = \langle \frac{3}{2}(\cos^2\theta) - \frac{1}{2} \rangle$ where θ is the angle between the carbon atom and the hydrogen (deuterium) atom and the bilayer normal, as shown in Fig. 2 (a). To show how 1-alkanols affect S_{cd} of the DOPC tails, we define $\delta S_{cd} = \frac{S_{cd}^0 - S_{cd}^A}{S_{cd}^0}$ where S_{cd}^A and S_{cd}^0 are the deuterium order parameter of the lipid chains, C_n of the DOPC-lipid bilayer membrane with and without 1-alkanol, respectively shown in Fig. 2 (b). There is a prominent deep in the value of S_{cd} at C_9 for all membranes without or with 1-alkanol shown in Fig. 2 (a) due to the double bond in the DOPC-lipid at 9th position of the acyl chain. Fig. 2 (b) shows that the value of δS_{cd} with C_n increases with longer acyl chain of the 1-alkanol. *Therefore, we find that the deuterium order parameter (S_{cd}) of the DOPC acyl chain decreases with chain length, n of the 1-alkanol acyl chain.*

C. Penetration of 1-alkanol

Fig. 3 shows the snapshot of 1-alkanol with varying chain length in the membrane at time, $t = 0$ ns, $t = 100$ ns, and $t = 1000$ ns, respectively which shows how the 1-alkanol with varying chain length differs in the penetration of the membrane. We collect the coordinates of the atoms in the head group of DOPC, entire DOPC lipids, and 1-alkanol molecules with time from the simulation of $1\mu s$ of DOPC with/ without 1-alkanols. We begin by calculating the lipid membrane's centre of mass (COM) ($x_{com}^{membrane}$, $y_{com}^{membrane}$, $z_{com}^{membrane}$) for each time frame. We also calculate the COM (x_{com} , y_{com} , z_{com}) of the head group of each lipid and that of the entire 1-alkanol molecule with time, respectively. With time, we form groups of DOPC lipids and 1-alkanol molecules that remain in the upper ($z_{com} > z_{com}^{membrane}$) and lower ($z_{com} < z_{com}^{membrane}$) leaflets, respectively. Now, we calculate the average COM of the head group of DOPC lipid and 1-alkanol of the upper and lower leaflet, respectively, averaged over the number of lipids/ 1-alkanol in each leaflet. The time evaluation of the z -component of the COM (z_{com}) of the head group of DOPC lipid and 1-alkanol of the upper and lower leaflet is shown in Fig. 4. The depth of the penetration, d_p of the 1-alkanol is defined as, $d_p^{upper(lower)} = |(z_{com}^{upper(lower)-dopc-head-group} - z_{com}^{upper(lower)-alkanol})|$. As shown in Fig. 5 (a), the penetration depth of 1-alkanols, d_p , increases with the value

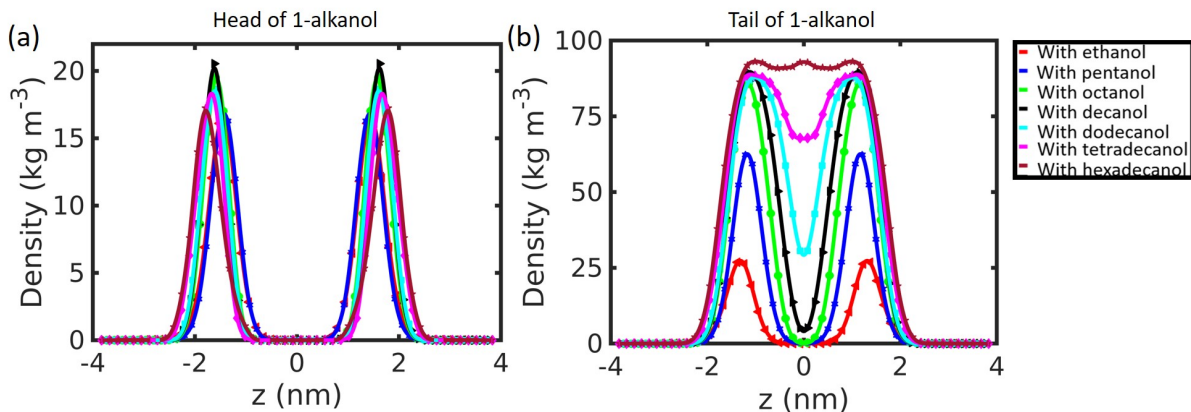


FIG. 1. The density profile of the head and tail of 1-alkanol in the DOPC bilayer, respectively are shown, where head group comprises with $-OH$ and tail group comprises with acyl chain, $-(CH_2)_{n-1} - CH_3$ with varying $n = 2, 5, 8, 10, 12, 14, 16$, respectively.

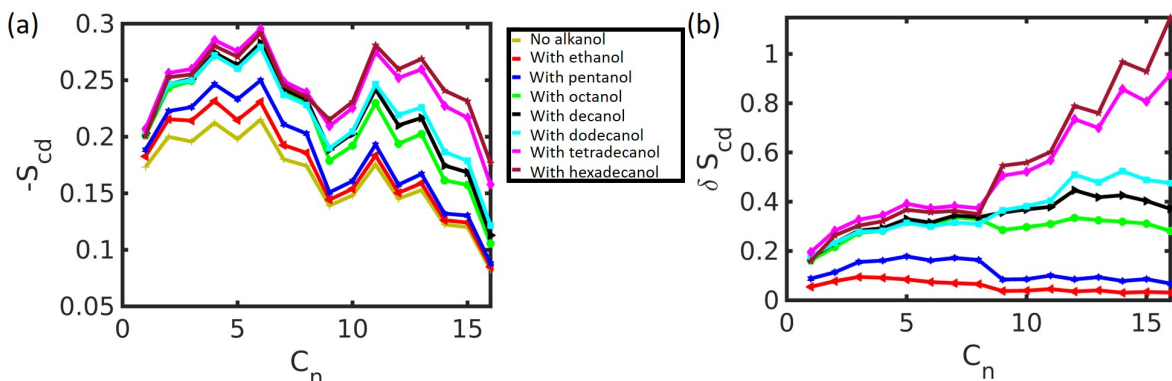


FIG. 2. The deuterium order parameter, S_{cd} and the fraction of the deuterium order parameter, δS_{cd} with the carbon number, C_n of the acyl chain of the DOPC of the bilayer membrane with 1-alkanol with varying acyl chain length, respectively are shown.

of acyl chain length, n . The time evaluation of the depth of penetration of 1-alkanol in the upper and lower leaflets and the mean value of them are shown in Fig. 4, where we highlight in color grey the value d_p of 1-alkanol in the bilayer membrane until it reaches the asymptotic values, which is denoted as the penetration time, τ_p of 1-alkanol. Fig. 5 (b) shows that the time of penetration of 1-alkanols with different acyl chains has a cut-off value, $n = 12$, below which 1-alkanol molecules can penetrate to the membrane within $100 - 200 ns$, but 1-alkanols with longer acyl chains take a long time (approximately $300 - 500 ns$). *As a result, we find that the penetration time of 1-alkanol has a cut-off value ($n = 12$) for the acyl chain of 1-alkanol, even though the depth of penetration of 1-alkanol increases with acyl chain length.*

D. Clusterization of 1-alkanols

To study the clusterization of 1-alkanol in the lipid membrane, we have developed a novel technique based on Matlab-image analysis tool fusion with the Voronoi tessellation technique. Our method can be widely applicable to the study of clusters of molecules in any molecular dynamics [32, 39, 41] or Monte Carlo simulation [42] as well as any experiments describing spatial heterogeneity of molecules such as fluorescent-based experiments (confocal FM, FRET, TIRF) [41] to study the spatial organisation of cell membrane components.

We use last $500 ns$ trajectory out of the entire $1000 ns$ simulation of each system, where we have saved each frame in a $100 ps$ interval during our simulation, and a total of 5000 frames of trajectory have been used to study clusterization of 1-alkanol. We collect the (x,y) positional coordinates of all 1-alkanol molecules for each frame and calculate the COM of each 1-alkanol molecule. The steps

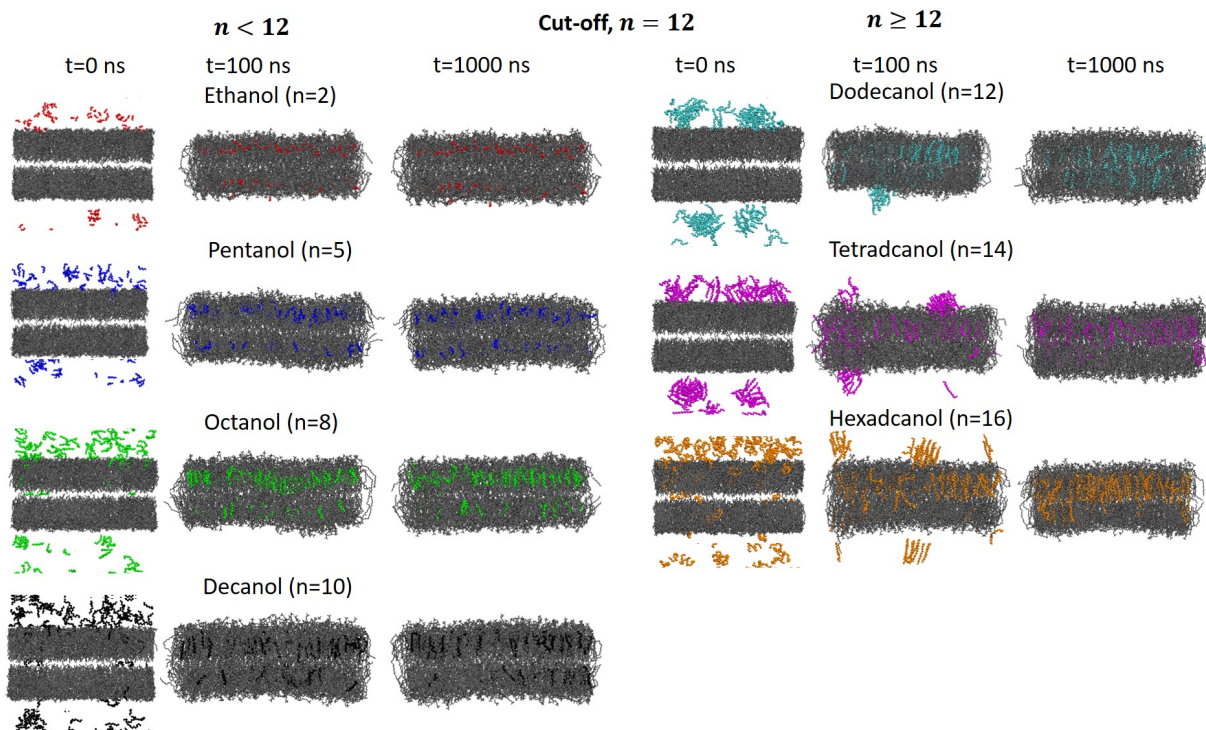


FIG. 3. The snapshot of the DOPC (grey) bilayer membrane with 1-alkanol with varying acyl chain length, $n = 2$ (red), 5 (blue), 8 (green), 10 (black), 12 (cyan), 14 (magenta), and 16 (orange) at different time, $t = 0 \text{ ns}$, $t = 100 \text{ ns}$, and $t = 1000 \text{ ns}$, respectively are shown.

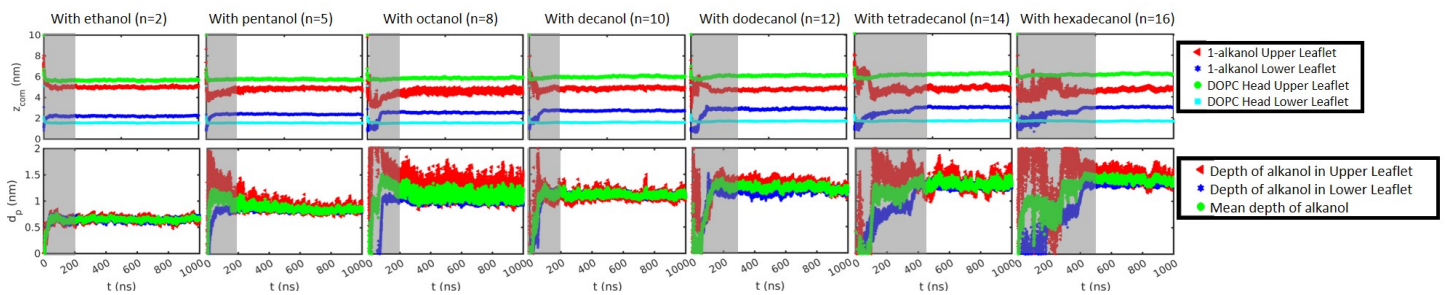


FIG. 4. The time evaluation of the z -component of the center of mass, z_{com} and the depth of penetration, d_p of the 1-alkanol in the DOPC bilayer membrane with 1-alkanol with varying acyl chain, respectively are shown.

to calculate the cluster of 1-alkanol in each frame are given below.

First, we plot the x and y -components of the COM of each 1-alkanol for each frame (For example, here, the spatial distribution of COM of each 1-alkanol is shown at time-frame $t = 1000 \text{ ns}$ in the left-most column figure in Fig. 6. Second, we use Voronoi tessellation technique to obtain Voronoi-diagram of 1-alkanol and highlight the Voronoi-cells with different colors corresponding to each 1-alkanol, as shown in the second column figure in Fig. 6. Third, from the Voronoi-cells of the 1-alkanol, we calculate the density by inverting the area of each cell, as each Voronoi-cell contains one 1-alkanol molecule, and we

calculate the mean density of the 1-alkanol. Now, only Voronoi-cells with densities greater than the mean density are selected and the Voronoi-cells in different colors with high densities are shown in the third column figure in Fig. 6. Fourth, as shown in the fourth column of Fig. 6, we fill-up all Voronoi-cells with higher density in white color while the regions of Voronoi-cells with lower density are shaded in black color, respectively and save them in high resolution ($\sim 1024p$). We notice that the white region in the figure is a cluster of 1-alkanol. Now, we read the high-resolution black-and-white image of the cluster in Matlab and use the function 'bwlabel' to calculate the area of the polygonal white space representing the cluster

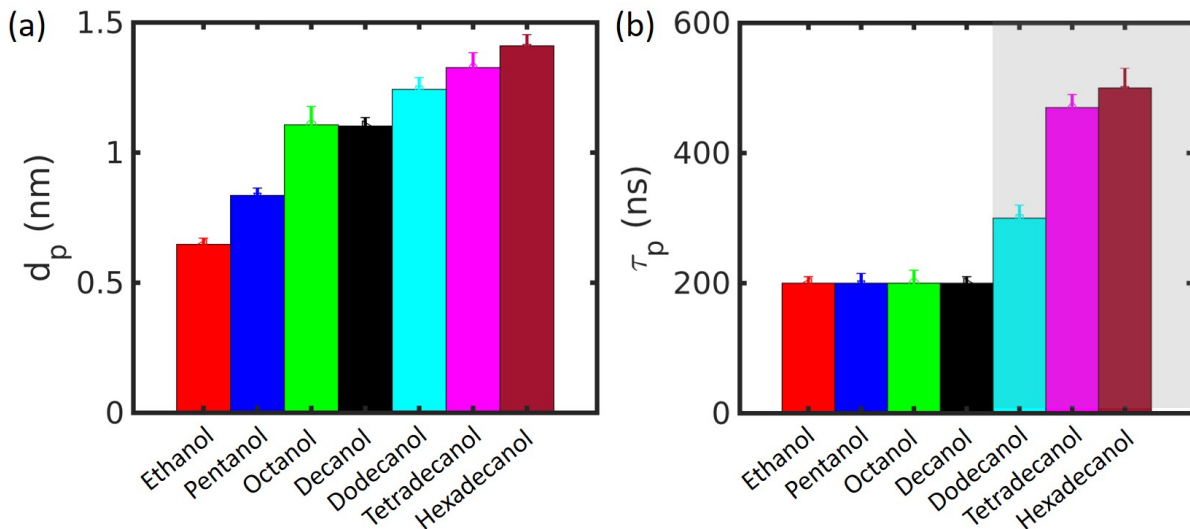


FIG. 5. The depth of penetration, d_p and the time of penetration, τ_p of the 1-alkanol in the DOPC bilayer membrane with 1-alkanol with varying acyl chain length, respectively are shown.

based on the pixels as a smallest bin-size of the image.

From all the frames in the last 500 ns trajectory of the simulation, we gather all the values of the area of clusters of 1-alkanol exhibited in each frame. We plot the probability distribution of the area of the cluster, $P(A_{cluster})$, shown in Fig. 7, which shows the formation of a distinct cluster only for 1-alkanol with an acyl chain ($n = 12, 14, \text{ and } 16$) at 20 nm^2 , 30 nm^2 , and 45 nm^2 , respectively. Thus, 1-alkanols with higher acyl-chain lengths ($n \geq 12$) exhibit prominent clusterization in lipid membranes, and there is no cluster exhibited for 1-alkanols with shorter acyl chains ($n < 12$). However, we need to use Voronoi tessellation on both the lipid and the 1-alkanol in the same frame and calculate the probability distribution of the area of the lipid and the 1-alkanol, and estimate the area as $0.5 \pm 0.1 \text{ nm}^2$ and $0.38 \pm 0.1 \text{ nm}^2$ for DOPC and the 1-alkanol, respectively, as shown in Fig. 7.

Therefore, we find that there is a cut-off value, $n = 12$, of the acyl chain length of 1-alkanol above which the hydrophobic effect of the acyl chains is strong enough to form a cluster of 1-alkanol.

We can calculate clusters of 1-alkanol from the spatial number density plot shown in Fig. 8 by dividing the system's box with 12×12 square grids with a bin-size 1 nm (considering, the size of the membrane is approximately $12 \times 12 \text{ nm}^2$) and then getting the high-density bins, which are denser than average, followed by cluster analysis. Our method, demonstrated above, is efficient compared to the square grid method. Using the Voronoi tessellation method, we get the actual polygonal area where the COM of molecules is present at the center and we obtain polygonal clusters of the 1-alkanols. Since there is a possibility that the borders of the bins will contain the COM of molecules, if we use the square grid

approach to calculate number density, we might run into artefacts. Furthermore, by analyzing a black-and-white image that is saved to define the the cluster of 1-alkanols, we improve our calculation for determining the properties of the cluster, because the smallest bin size in our method is the size of a pixel in the image.

E. Radial distribution

We calculate the radial distribution, $g(r)$, of the pair distance between two 1-alkanols and that of the pair distance between 1-alkanol - DOPC lipid, as shown in Fig. 9 (b) and (c), respectively, for varying acyl chain length, n , of 1-alkanol. In dodecanol, tetradecanol, and hexadecanol, there are prominent peaks at 0.5 nm in the $g(r)$ of the 1-alkanol—1-alkanol pair shown in Fig. 9 (b), which are very small in ethanol, pentanol, octanol, and decanol. Because of the strong hydrophobic effect of the long acyl chains, the 1-alkanol with a long acyl chain ($n \geq 12$) interacts with itself and forms clusters. Short acyl chain 1-alkanols, on the other hand, do not form clusters due to low hydrophobic interaction. Fig. 9 (c) shows prominent peaks in the $g(r)$ of the 1-alkanol-DOPC pair at 0.25 nm for ethanol, pentanol, octanol, and decanol, respectively indicating comparatively higher interaction with lipids, which are absent for dodecanol, tetradecanol, and hexadecanol. Thus, 1-alkanol with a short chain acyl chain is homogeneously distributed in the membrane, as shown in Fig. 6, and can penetrate the lipid membrane easily due to its small size while it takes a long time for a lump of clustered 1-alkanol to penetrate the membrane.

Therefore, 1-alkanols with a higher acyl chain length ($n \geq 12$) interact together more than that of a lipid, lead-

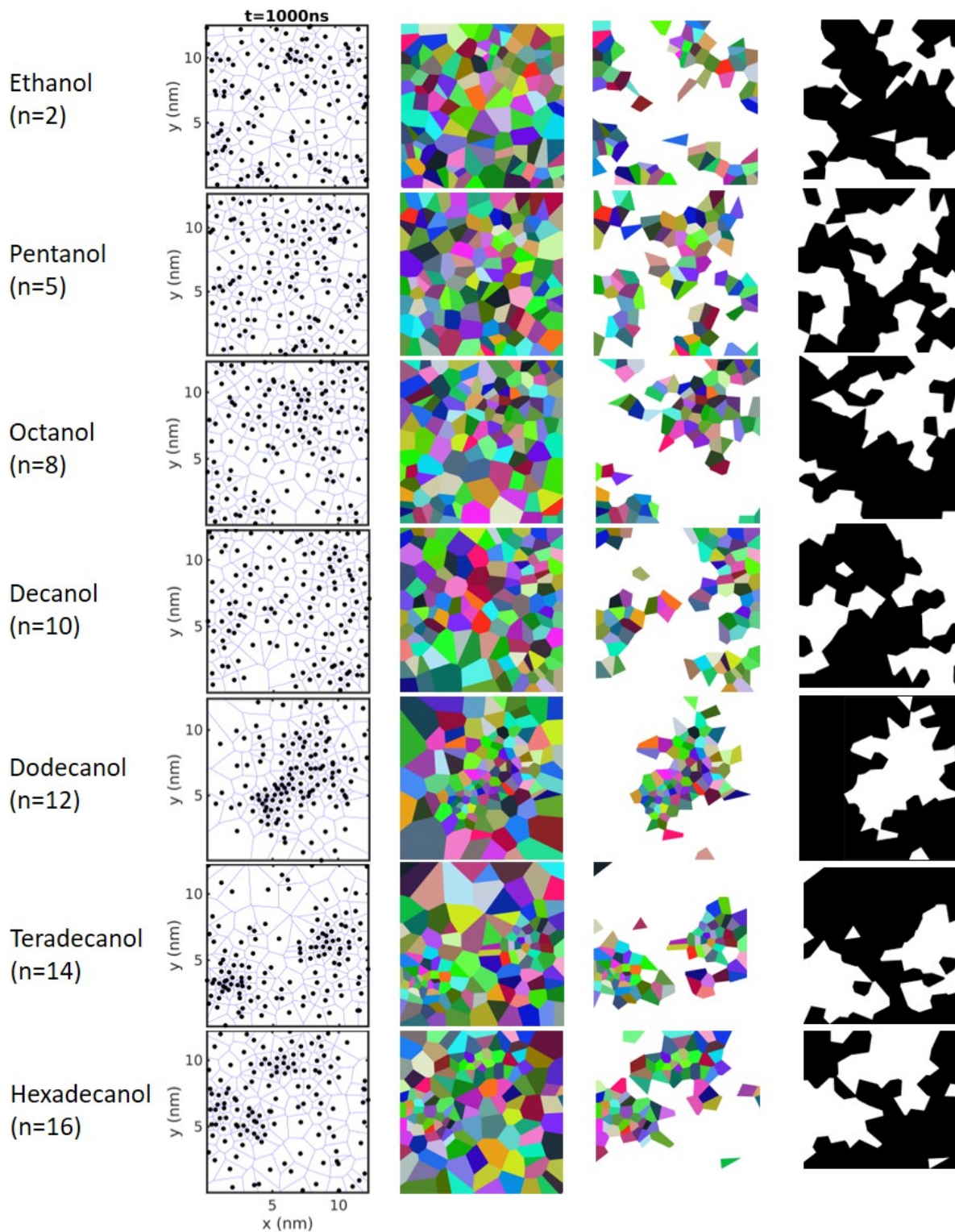


FIG. 6. The clusterization of 1-alkanols using Voronoi Tessellation technique are shown for the 1-alkanol (black circle) in the DOPC bilayer membrane with varying acyl chain length, respectively are shown.

ing to the formation of cluster and take a long penetration time, while 1-alkanols with a lower acyl chain length ($n < 12$) interact with lipids less than that of themselves,

are distributed uniformly in the membrane, and take a shorter penetration time.

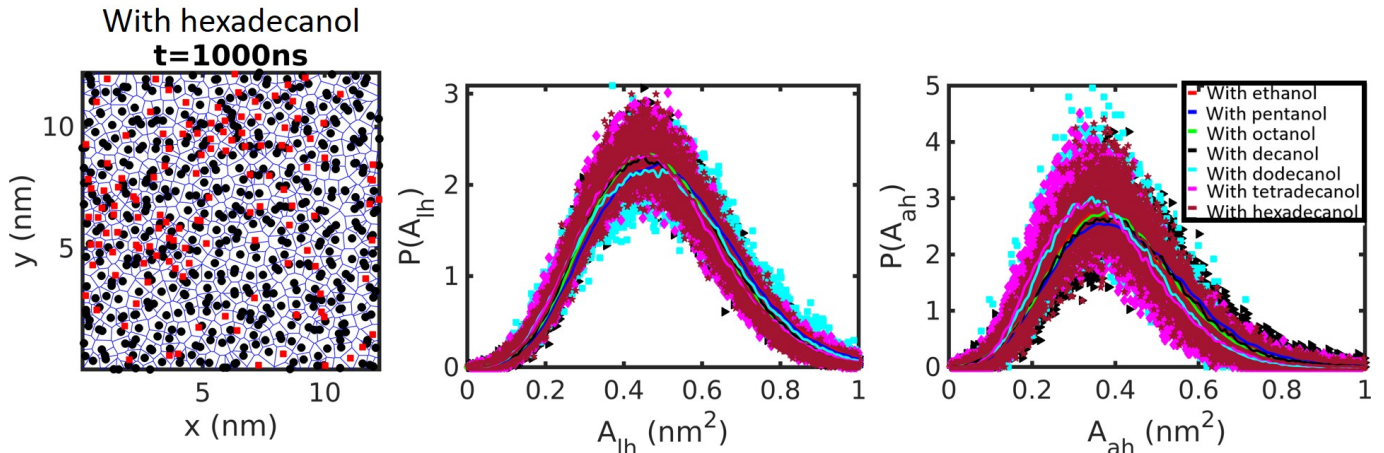


FIG. 7. The Voronoi diagram of the center of mass of the hexanol (red square) and DOPC lipid (black circle) together at time, $t = 1000 ns$ and the probability distribution of the area per lipid and 1-alkanol for the bilayer membrane with 1-alkanol with varying acyl chain, respectively are shown.

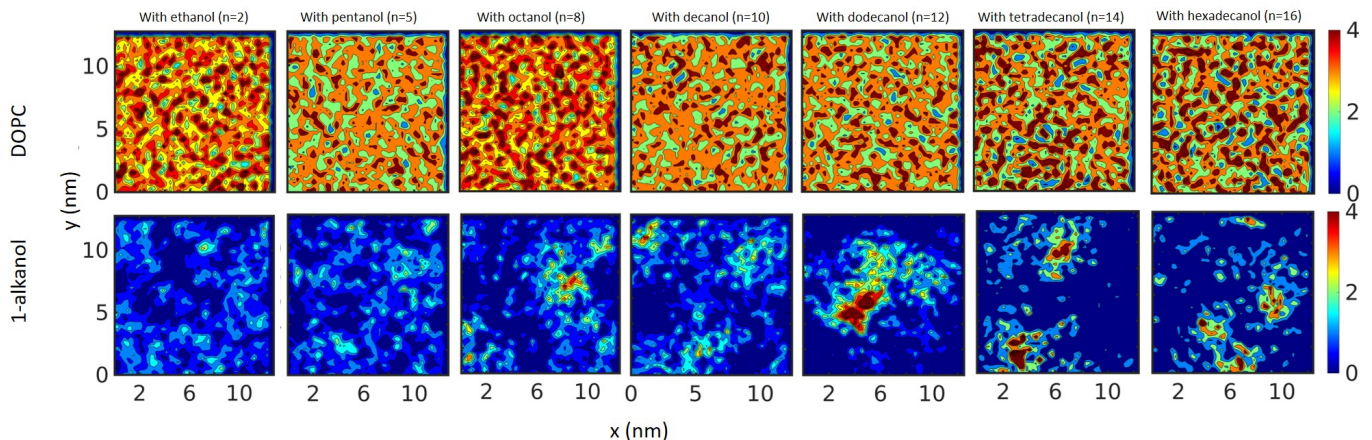


FIG. 8. The number density of the DOPC and 1-alkanol averaged over last 500 ns trajectory of the entire simulation of $1 \mu s$ of the DOPC bilayer membrane with 1-alkanol with varying acyl chain, respectively are shown.

IV. CONCLUSION

We present the effect of 1-alkanols with different chain lengths in the symmetric bilayer membrane comprising DOPC using atomistic molecular dynamics simulation. Here, we explore the effects of 1-alkanols with varying chain length in the membrane. Our main findings in the present study are the following: the depth of penetration of 1-alkanol into the membrane increases with the chain length (n) of the acyl chain of the 1-alkanol. The deuterium order parameter (S_{cd}) of the DOPC acyl chain, C_n , increases with the length of the 1-alkanol acyl chain. We find a cut-off value ($n = 12$) of the acyl chain length of the 1-alkanol, above which the membrane exhibits clusters of the 1-alkanol due to higher interaction among themselves. As a result, 1-alkanols with an acyl

chain with a higher cut-off value take longer to penetrate the membrane, as the lump of 1-alkanols requires more time to get enough space to penetrate the membrane. 1-alkanols with short chain lengths, on the other hand, are distributed uniformly in the membrane and interact with lipids in the membrane, penetrating the membrane in a short period of time due to their small size. This could explain why 1-alkanol with a shorter acyl-chain is more effective as an anesthetic.

Our findings show that both the penetration depth and time of 1-alkanol molecules into the membrane vary with their acyl chain length and could be useful for the study of 1-alkanols and their anesthetic effects.

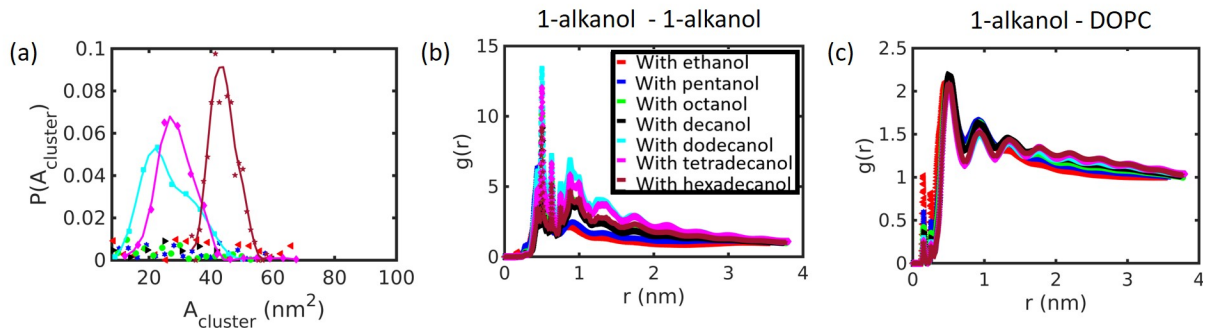


FIG. 9. The Probability distribution of the area of clusterization, $P(A_{cluster})$ of 1-alkanols are shown in Fig9 (a) for the 1-alkanol in the DOPC bilayer membrane with varying acyl chain length, respectively. The radial distribution, $g(r)$ of the 1-alkanol - 1-alkanol pair and 1-alkanol - DOPC pair for the 1-alkanol in the DOPC bilayer membrane with varying acyl chain length are shown Fig9 (b) and (c), respectively.

ACKNOWLEDGMENTS

A.P. gratefully acknowledges the hospitality of generous the computing facilities of clusters at SASTRA Uni-

versity, Thanjavur, Tamilnadu. A.P. acknowledges the support under Science and Engineering Research Board (SERB), Department of science and technology, Government of India [SERB-SRG/2022/001489] and T.R. Rajagopalan research fund, SASTRA University, India.

-
- [1] P. Seeman, “The membrane actions of anesthetics and tranquilizers.” *Pharmacol Rev.* **24**, 583 (1972).
- [2] N. P. Franks and W. R. Lieb, “Molecular and cellular mechanisms of general anaesthesia,” *Nature* **367**, 607 (1997).
- [3] N. P. Franks and W. R. Lieb, “Selectivity of general anesthetics: A new dimension.” *Nat. Med.* **3**, 377 (1997).
- [4] S. Turkyilmaz, W. H. Chen, H. Mitomo, and S. L. J. Regen, “Loosening and reorganization of fluid phospholipid bilayers by chloroform.” *J. Am. Chem. Soc.* **131**, 5068 (2009).
- [5] I. Ueda and A. Suzuki, “Does pressure antagonize anesthesia? opposite effects on specific and nonspecific inhibitors of firefly luciferase.” *Biophys. J.* **75**, 1052 (1998).
- [6] I. Ueda and A. Suzuki, “Molecular mechanisms of anesthesia.” *Keio J. Med.* **50**, 20 (2001).
- [7] J. Alifimoff, L. Firestone, and K. W. Miller, “Anaesthetic potencies of primary alkanols: implications for the molecular dimensions of the anaesthetic site.” *Br J Pharmacol.* **96**, 9 (1989).
- [8] S. E. Feller, C. A. Brown, D. T. Nizza, and K. Gawrisch, “Nuclear overhauser enhancement spectroscopy cross-relaxation rates and ethanol distribution across membranes.” *Biophys. J.* **82**, 15 (2002).
- [9] L. Holte and K. Gawrisch, “Determining ethanol distribution in phospholipid multilayers with mas-noesy spectra.” *Biochem.* **36**, 4669 (1997).
- [10] J. A. Barry and K. Gawrisch, “Effects of ethanol on lipid bilayers containing cholesterol, gangliosides and sphingomyelin.” *Biochem.* **34**, 8852 (1995).
- [11] M. Patra, E. Salonen, E. Terama, I. Vattulainen, R. Faller, B. W. Lee, J. Holopainen, and M. Karttunen, “Under the influence of alcohol: the effect of ethanol and methanol on lipid bilayers.” *Biophys. J.* **90**, 1121 (2006.).
- [12] J. T. Marquês, A. S. Viana, and F. M. Rodrigo de Almeida, “Ethanol effects on binary and ternary supported lipid bilayers with gel/fluid domains and lipid rafts.” *Biochim. Biophys. Acta.* **1808**, 405 (2011).
- [13] I. Vorobyov, W. F. Drew Bennett, P. D. Tieleman, T. W. Allen, and S. Noskov, “The role of atomic polarization in the thermodynamics of chloroform partitioning to lipid bilayers.” *J. Chem. Theory. Comput.* **8**, 307 (2012).
- [14] R. S. Cantor, “The lateral pressure profile in membranes: a physical mechanism of general anesthesia.” *Biochem.* **36**, 2339 (1997).
- [15] R. S. Cantor, “Lateral pressures in cell membranes: a mechanism for modulation of protein function.” *J. Phys. Chem. B* **101**, 1723 (1997).
- [16] R. S. Cantor, “The lateral pressure profile in membranes: a physical mechanism of general anesthesia.” *Toxicol. Lett.* **100**, 451 (1998).
- [17] A. Polley and S. Vemparala, “Partitioning of ethanol in multi-component membranes: Effects on membrane structure.” *Chem Phys Lipids.* **166**, 1 (2013).
- [18] J. Chanda and S. Bandyopadhyay, “Distribution of ethanol in a model membrane: a computer simulation study.” *Chem. Phys. Lett.* **392**, 249 (2004).
- [19] J. Chanda and S. Bandyopadhyay, “Perturbation of phospholipid bilayer properties by ethanol at a high concentration.” *Langmuir* **22**, 3775 (2006).
- [20] M. Kranenburg and B. Smit, “Simulating the effect of alcohol on the structure of a membrane.” *FEBS Lett.* **568**, 15 (2004).
- [21] E. Terama, O. H. Ollila, E. Salonen, A. C. Rowat, C. Trandum, P. Westh, M. Patra, M. Karttunen, and I. Vattulainen, “Simulating the effect of alcohol on the structure of a membrane.” *J. Phys. Chem. B.* **112**, 4131 (2008).

- [22] B. Griepernau, S. Leis, M. F. Schneider, M. Sikor, D. Steppich, and R. A. Böckmann, "1-alkanols and membranes: a story of attraction." *Biochim. Biophys. Acta.* **1768**, 2899 (2007).
- [23] R. Dickey, A. N. and Faller, "How alcohol chain-length and concentration modulate hydrogen bond formation in a lipid bilayer." *Biophys. J.* **92**, 2366 (2007).
- [24] U. Vierl, L. Lobbecke, N. Nagel, and G. Cevc, "Solute effects on the colloidal and phase behavior of lipid bilayer membranes: ethanol-dipalmitoylphosphatidylcholine mixtures." *Biophys. J.* **67**, 1067 (1994).
- [25] T. Heimburg and A. D. Jackson, "The thermodynamics of general anesthesia." *Biophys. J.* **92**, 3159–3165 (2007).
- [26] J. A. Barry and K. Gawrisch, "Effects of ethanol on lipid bilayers containing cholesterol, gangliosides, and sphingomyelin." *Biochem.* **34**, 8852 (1995).
- [27] C. W. Hollars and R. C. Dunn, "Submicron structure in 1-alpha-dipalmitoylphosphatidylcholine monolayers and bilayers probed with confocal, atomic force, and near field microscopy." *Biophys. J.* **75**, 342 (1998).
- [28] S. A. Simon and T. J. McIntosh, "Interdigitated hydrocarbon chain packing causes the biphasic transition behavior in lipid alcohol suspensions." *Biochim. Biophys. Acta.* **773**, 169 (1984).
- [29] E. Lindahl, B. Hess, and D. van der Spoel, "Gromacs 3.0: a package for molecular simulation and trajectory analysis," *Journal of Molecular Modeling* **7**, 306 (2001).
- [30] L. Martínez, R. Andrade, E. Birgin, and J. Martínez, "Packmol: a package for building initial configurations for molecular dynamics simulations." *J Comput Chem.* **30(13)**, 2157 (2009).
- [31] J. de Joannis, P. S. Coppock, F. Yin, M. Mori, A. Zamorano, and J. T. Kindt, "Atomistic simulation of cholesterol effects on miscibility of saturated and unsaturated phospholipids: implications for liquid-ordered/liquid-disordered phase coexistence." *J Am Chem Soc.* **133**, 3625 (2011).
- [32] A. Polley, S. Vemparala, and M. Rao, "Atomistic simulations of a multicomponent asymmetric lipid bilayer." *J Phys Chem B.* **116(45)**, 13403 (2012).
- [33] D. P. Tieleman and H. J. Berendsen, "A molecular dynamics study of the pores formed by escherichia coli ompf porin in a fully hydrated palmitoyloleoylphosphatidylcholine bilayer." *Biophys J.* **74(6)**, 2786 (1998).
- [34] P. S. Niemelä, S. Ollila, M. T. Hyvönen, M. Karttunen, and I. Vattulainen, "Assessing the nature of lipid raft membranes," *PLoS Comput Biol.* **3(2)**, e34 (2007).
- [35] B. Griepernau and R. A. Böckmann, "The influence of 1-alkanols and external pressure on the lateral pressure profiles of lipid bilayers." *Biophys J.* **95**, 5766 (2008).
- [36] M. Patra, E. Salonen, E. Terama, I. Vattulainen, R. Faller, B. W. Lee, J. Holopainen, and M. Karttunen, "Under the influence of alcohol: The effect of ethanol and methanol on lipid bilayers." *Biophys. J.* **90**, 1121 (2006).
- [37] R. Reigada, "Influence of chloroform in liquid-ordered and liquid-disordered phases in lipid membranes." *J. Phys. Chem. B.* **115**, 2527 (2011).
- [38] R. Reigada, "Atomistic study of lipid membranes containing chloroform: Looking for a lipid-mediated mechanism of anesthesia." *PLoS Comput Biol.* **8**, e52631 (2013).
- [39] A. Polley, S. Mayor, and M. Rao, "Bilayer registry in a multicomponent asymmetric membrane: dependence on lipid composition and chain length," *J. chem. physics.* **141**, 064903 (2014).
- [40] M. Patra and M. Karttunen, "Lipid bilayers driven to a wrong lane in molecular dynamics simulations by subtle changes in long-range electrostatic interactions," *J. Phys. Chem. B* **108 (14)**, 4485 (2004).
- [41] R. Raghupathy, A. A. Anilkumar, A. Polley, P. P. Singh, M. Yadav, C. Johnson, S. Suryawanshi, V. Saikam, S. D. Sawant, A. Panda, Z. Guo, R. A. Vishwakarma, M. Rao, and S. Mayor, "Transbilayer lipid interactions mediate nanoclustering of lipid-anchored proteins," *Cell* **161 (3)**, 581 (2015).
- [42] A. Das, A. Polley, and M. Rao, "Phase segregation of passive advective particles in an active medium," *Phys. Rev. Lett.* **116**, 068306 (2016).

The understanding of the penetration and clusterization of 1-alkanol in bilayer membrane: An open outlook based on atomistic molecular dynamics simulation

Anirban Polley*

*Shanmugha Arts, Science, Technology and Research Academy,
Tirumalaisamudram, Thanjavur, Tamilnadu 613401, India*

(Dated: June 2, 2025)

SUPPLEMENTARY INFORMATION

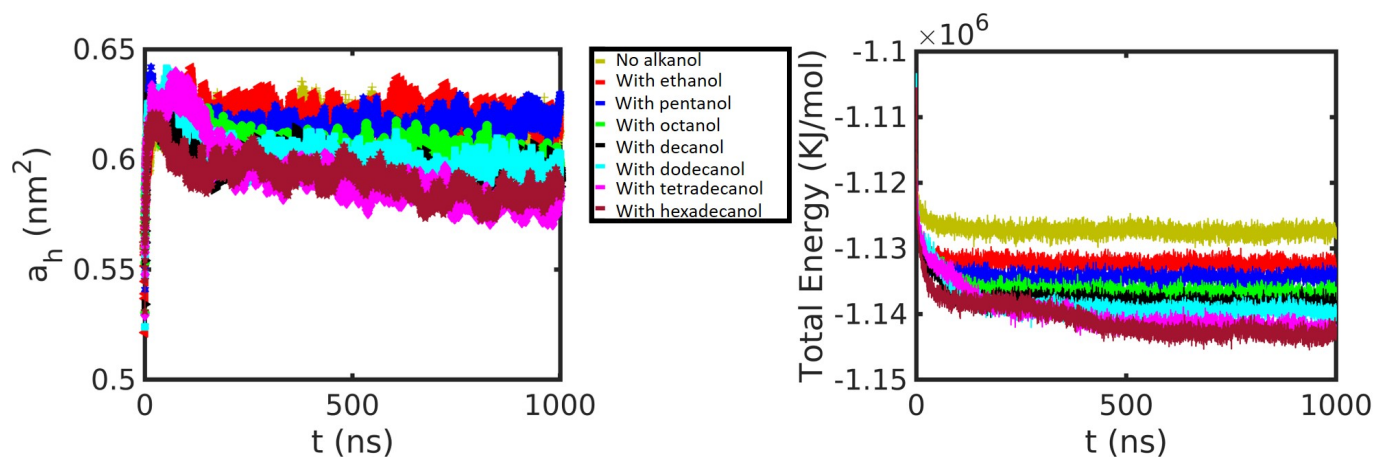


FIG. S1. The time evaluation of the average area per head of the DOPC lipid calculated by the number of DOPC for each leaflet divided by the area of the xy -plane of the box size and the time evaluation of energy of the DOPC bilayer membrane without and with 1-alkanol with varying acyl chain, respectively are shown.

* anirban.polley@gmail.com

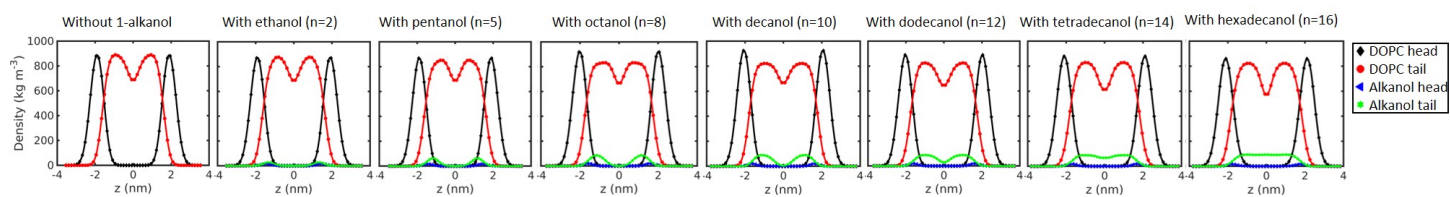


FIG. S2. The density profile of the head and tail of DOPC and 1-alkanol for the DOPC bilayer membrane without and with 1-alkanol with varying acyl chain, respectively are shown.